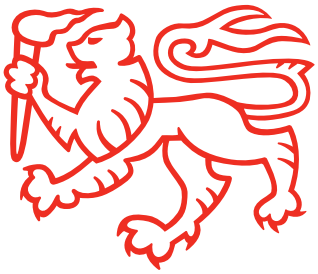

UNIVERSITY of TASMANIA

PART II LABORATORY WORK

KYA 211/212

Time Domain Reflectometry (TDR)

Last compiled 2026-04-02

Safety

The time domain refractometry lab uses a variety of electrical cables. Always inspect cables and connectors for damage before use. Report any damage to your demonstrator.

Be sure to keep long cables in their spools to avoid trip hazards.

Outline

Summary

This experiment explores the properties of waveforms propagating through cables with different characteristic impedances. By examining the behaviour of reflected waves at boundaries with high, low, and matched impedance, we relate these reflections to the wave equation. Additionally, the characteristic impedance and pulse propagation speed in the cable are measured and used to determine the cable's inductance and capacitance, which are then compared to theoretical predictions.

Experiment Objectives

- **Primary:** To compare the characteristic inductance and capacitance of the cables derived from measurements of the pulse speed and impedance to the theoretically predicted values.
- **Secondary:** To study the effect of matched impedance on pulse reflections and to observe and record the waveforms associated with reflections off of barriers with varying characteristic impedances.

Pre-lab Exercises

Pre-lab questions should be completed and submitted before you commence a new experiment. The information needed to complete the exercises is contained in the Background Theory Section, your course notes, or in the Appendices however, your own, independent research is highly encouraged. Make sure you include references where material has been sought elsewhere. This is not only "good form" but making notes of important information is essential if you then need to go back to that reference.

Task

1. TDR traces of transmission lines are not only used to determine where a discontinuity is, but identify the type of discontinuity. The below figure shows a sketch of a TDR trace of a transmission line, showing the transmitted signal and then reflected signal. Panel (a) shows the signal reflected from an open termination, while (b) displays the reflection from a short circuit termination. Describe why the magnitudes of the reflections are opposing. Use relevant equations to support your answer.

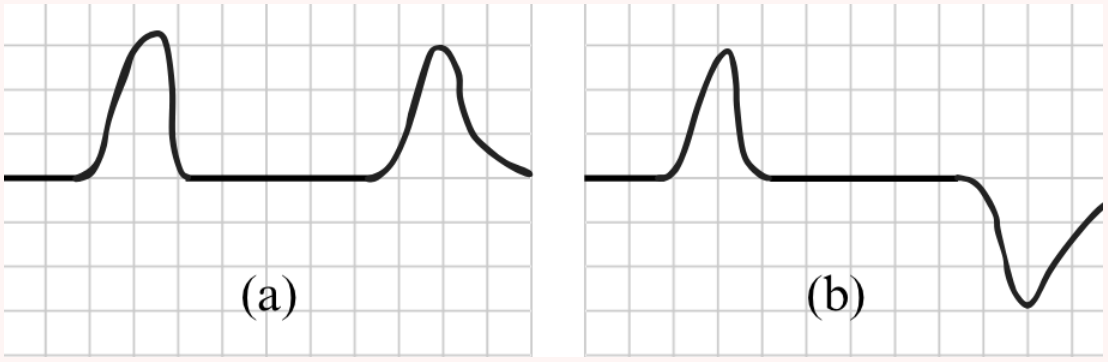

2. Using the definitions of capacitance and inductance together with the geometry in Figure 1 (a), derive Equations 4 and 5 which describe the capacitance per unit length and inductance per unit length for a coaxial cable.

3. TDR has a plethora of real-world applications. The appendix contains a paper by Topp et al. (1980) which was among the first to apply the principles of TDR to analysing the water content in soils. With this paper as a reference, explain the relationship between soil water content and the dielectric constant. Why is the dielectric constant sensitive to changes in water content?

Background Theory

Overview of TDR

Time Domain Reflectometry (TDR) is a technique that uses the reflection of electrical pulses sent through a conductor (such as electrical cables) to analyze the characteristics, faults, or discontinuities in the conductor. As the pulse travels down the cable, any discontinuity (change in the characteristic impedance) will result in some or all of the incident signal being reflected. In the context of cable testing, such a reflection means a fault in the line. By analysing the time between the initial pulse and the detection of the reflections, the spatial location of the fault can be determined using the known propagation velocity of the waves.

As a method for cable testing, the TDR technique has been used for almost one hundred years. In the 1930s it became a recognised technique in cable testing and was widely used by the 1960s as a method to determine the dielectric properties of transmission lines (Fellner-Feldegg, 1969).

The applications of TDR have since stretched far beyond simply finding faults in cables. Al-Qadi et al. (1997) used TDR to determine the dielectric properties of portland cement concrete, while research by Davis (1975), Topp et al. (1980) and Patterson and Smith (1980) were among the first studies that applied TDR methods to determine the volumetric water content of a porous medium like soil. Nowadays, TDR is the most widely-used non-destructive method for the measurement of soil water content. In this lab, we are interested in TDR methods applied to transmission lines, and so we shall now explore this further.

TDR with Transmission Lines

An electromagnetic signal in a wire is a form of wave, with its propagation speed and dispersive properties determined by the medium in which the wave travels. For a wire, these properties are typically summarised by a few related measurable properties: the characteristic impedance Z_0, the inductance per unit length (L') and the capacitance per unit length (C'); these are determined by the geometry and dielectric properties of the wire and any associated shielding.

In general, when a signal crosses from one wire to another, or encounters a junction, device, or break in the wire, a reflected pulse is generated because the signal "sees" the change in medium as an increase or decrease in Z_0. In the ideal case, when no energy is lost to dissipative effects, the expression relating the incident and reflected pulse voltage is

$$\frac{V_r}{V_i} = \frac{Z_L - Z_0}{Z_L + Z_0}, \tag{1}$$

where V_i and V_r are the incident and reflected voltages respectively, and Z_L is the load impedance (impedance of the barrier, device or new wire). The ratio V_i/V_r is often termed the voltage reflection coefficient, ρ. Clearly, the voltage of the reflected pulse can be very high, near zero, or even negative, depending on the relationship between Z_0 and Z_L. Equation 1 can be transformed into the equivalent equation for the current using Ohm's law.

In this lab you will encounter coaxial and twisted pair cables. These can be modeled in circuit theory as a long "ladder" formed by two wires with some series inductive impedance per unit length along the two wires and some

parallel capacitive impedance per unit length across the "rungs" of the ladder. This formulation leads to a description of the change in voltage and current with distance along the transmission line (dV/dx and dI/dx), the solution of which yields a wave equation in V (and in I).

For a single wave solution in one direction, the solution of the wave equation with the characteristic impedance Z_0 eventually gives:

$$Z_0 = \frac{V}{I} = \sqrt{\frac{L'}{C'}}. \tag{2}$$

In a lossless transmission line whose length is much shorter than the wavelength of the signal, the inductance per unit length L' can be determined from the definition of inductive reactance and the relationship between frequency, wavelength and wave velocity v. The complete derivation is given in Terman, 1955, (Chapter 4). For the purposes of this lab, the result of greatest interest is

$$L' = \frac{Z_0}{v}. \tag{3}$$

Equations 2 and 3 can be combined to derive a similar expression relating C' to v and Z_0. Using these equations allows the derivation of C' and L from measurements of the pulse v and Z_0.

C' and L' are ultimately determined by the construction of the transmission line. A coaxial cable consists of a solid conducting cylinder separated from a hollow cylindrical conductor by a dielectric material as shown in Figure 1. For inner and outer radii a and b respectively, the properties of the cable are given by:

$$C' = \frac{2\pi\kappa\epsilon_0}{\ln(b/a)} \tag{4}$$

$$L' = \frac{\mu_0}{2\pi}\ln(b/a) \tag{5}$$

where κ is the dielectric constant of the insulator and ϵ_0 and μ_0 are the permittivity and permeability of free space, with their usual values.

Because the twisted-pair wire has a different geometry, the transmission properties are quite different, and are given by

$$C' = \frac{\pi\kappa\epsilon_0}{\cosh^{-1}(s/2r)} \tag{6}$$

$$L' = \frac{\mu_0}{\pi}\cosh^{-1}(s/2r) \tag{7}$$

In this case the two wires have radius r and are separated by a fixed thickness s of insulating material, as seen in Figure 1. $\cosh^{-1}$ is the inverse hyperbolic cosine function, which may not be available on a typical hand calculator but is defined in most spreadsheet programs and coding packages such as python. In transmission lines comprising multiple pairs in parallel, the formula must be modified using the rules for combining impedances in parallel. This may become important depending on which twisted-pair wire you are using. For example, the burglar alarm used in this lab comprises two pairs of twisted strands, which are combined in parallel by the connectors at the cable ends. In Figure 1, imagine a second pair oriented 90^o away from the wires shown.

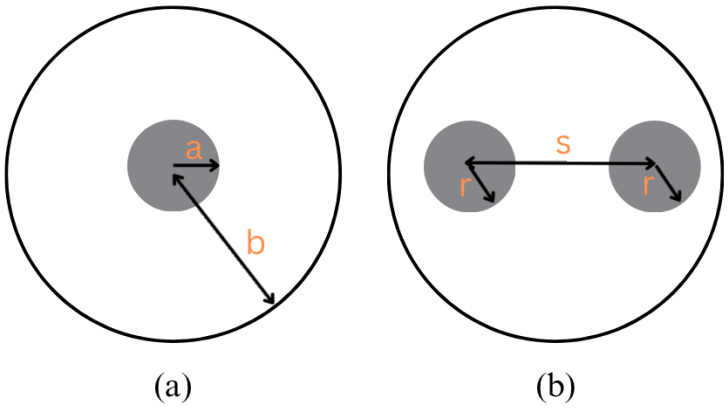

Figure 1: Cross-sections of a coaxial cable (a) and a twisted-pair (single-pair) wire (b).

Apparatus

To do this experiment, you will need the following components. A labelled diagram of the setup is shown in figure 2.

- Signal generator
- Oscilloscope
- Potentiometer (three terminal voltage divider)
- Transmission lines
  - coaxial cable
  - twisted pair wire
- Multimeter
- T-junction connectors
- BNC to banana plug leads - these allow you to create open and closed circuits.

The properties of each of the cables will be written on them (between 40 and $\approx$ 300 m). Cable length may be assumed to be accurate to ± 0.1 m. There will be multiple coaxial cables and twisted pair wires with slightly different characteristic impedances, lengths, and physical constructions (e.g. a single pair of conductors vs. a double pair in parallel). Make sure you note the properties of the cables you select and remain consistent throughout the experiment.

	Coaxial Cable	Telephone Wire	Burglar alarm
insulator dielectric constant, κ	2.3 ± 0.1 (high-density polyethylene)	2.3 ± 0.1	4.3 ± 0.1 (PVC)
inner diameter, a	0.90 ± 0.05 mm	-	-
outer diameter, b	3.80 ± 0.05 mm	-	-
pair separation, s	-	0.90 ± 0.05 mm	1.05 ± 0.05 mm
wire diameter, $2r$	-	0.52 ± 0.02 mm	0.54 ± 0.02 mm

Table 1: Transmission line properties.

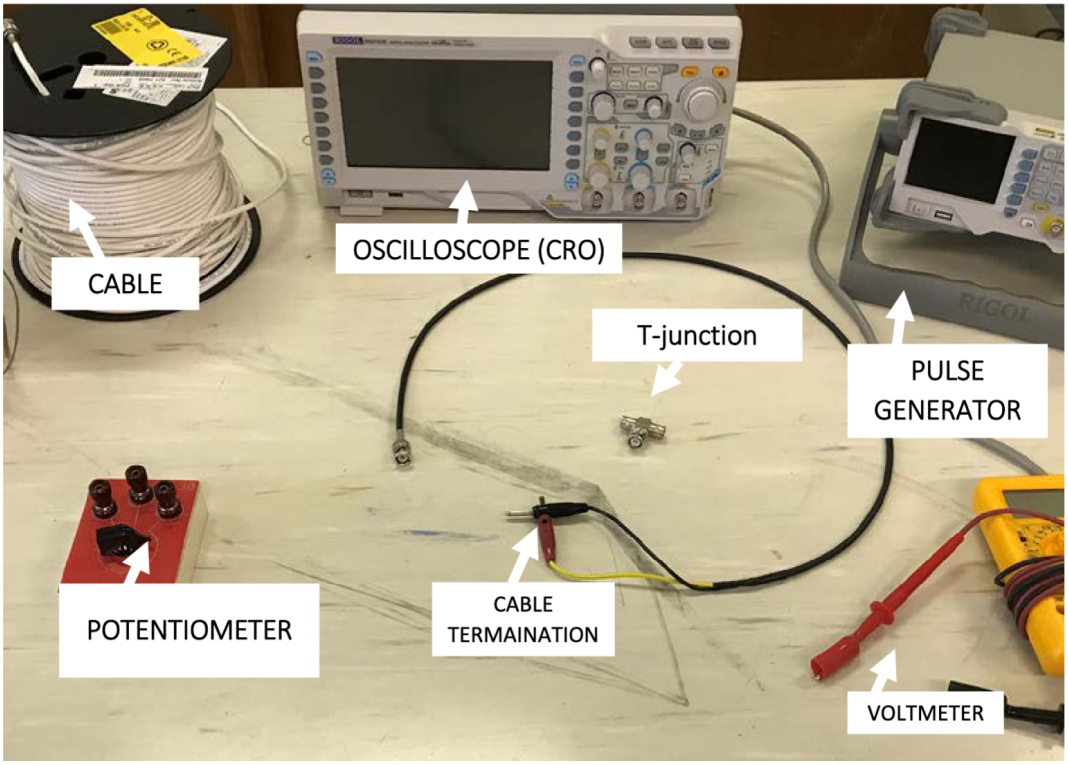

Figure 2: A labelled diagram of the key components used in the TDR lab.

Procedure

With the apparatus described and the relevant physics discussed, it is now time to design and execute the experiment that achieves the Experiment Objectives.

Task

Create an experiment plan that allows you to calculate values for the propagation speed v and the characteristic impedance Z_0 for two types of transmission line. When planning, it may help to think about the following questions?

1. Which two transmission lines will you use?
2. How should the signal generator, oscilloscope, and transmission lines be connected so you can see the transmitted and reflected pulse?
3. What wave properties (pulse width and cycle time, etc) should you set on the signal generator?
4. How can you measure the propagation speed of the pulse down the wire with the equipment you have? The oscilloscope has functions which will assist you
5. How will you be able to calculate the characteristic impedance? What features might you look for on the oscilloscope to indicate that the impedance is matched?
6. What are the likely sources of error in this experiment? Are some of them within your control? If so, how might you mitigate these?

Write down an outline of your experiment plan and discuss with your demonstrator before commencing.

While carrying out your experiment, remember to include the following in your logbooks

1. Labelled diagrams of your setup.
2. Details of your process including processes which didn't end up working out.
3. Assumed values.
4. Sources of error.
5. Sanity checks to validate your initial observations and any preliminary results. In other words, how do you know you're on the right track before you get to your final results?

Calculations and Discussion

Having accumulated your data, you can now derive the characteristic inductance and capacitance of the pulse speed and impedance and compare these to the theoretically predicted values.

Task

For both the cables you have tested complete the following:

1. Using your recorded values of the propagation velocity v and Z_0, determine L' and C' for the transmission line. It may be useful to remember that the units of L' and C' are henries per metre (M m^{-1}) and farads per metre (F m^{-1}), respectively.
2. Using the cable specifications, look up the characteristic impedance of the coaxial cable. Does the value agree with what you have measured?
3. Using the relevant equations for calculating C' and L', determine the *expected* values for L' and C' for the transmission lines you have used. Do your empirically determined values agree with the theory?

As you process your results, remember to **propagate your errors and display error bars on key plots.**

References

Al-Qadi, I., Riad, S., Mostaf, R. and Su, W. (1997), 'Design and evaluation of a coaxial transmission line fixture to characterize portland cement concrete', *Construction and Building Materials* **11**(3), 163–173.

Davis, J. (1975), 'Relative permittivity measurements of a sand and clay soil in situ', *Geological Survey Canada, Ottawa* pp. 75–1C.

Fellner-Feldegg, H. (1969), 'Measurement of dielectrics in the time domain', *The Journal of Physical Chemistry* **73**(3), 616–623.

Patterson, D. and Smith, M. (1980), 'The use of time domain reflectometry for the measurement of unfrozen water content in frozen soils', *Cold Regions Science and Technology* **3**(2-3), 205–210.

Terman, F. E. (1955), *Electronic And Radio Engineering, 4th Edition*, McGraw-Hill.

Topp, G. C., Davis, J. L. and Annan, A. P. (1980), 'Electromagnetic determination of soil water content: Measurements in coaxial transmission lines', *Water Resources Research* **16**(3), 574–582.

Appendices

WATER RESOURCES RESEARCH, VOL. 16, NO. 3, PAGES 574–582, JUNE 1980

Electromagnetic Determination of Soil Water Content: Measurements in Coaxial Transmission Lines

G. C. TOPP

Land Resource Research Institute, Agriculture Canada, Ottawa, Canada K1A OC6

J. L. DAVIS[1] AND A. P. ANNAN[2]

Geological Survey of Canada, Energy, Mines and Resources Canada, Ottawa, Canada K1A OE8

The dependence of the dielectric constant, at frequencies between 1 MHz and 1 GHz, on the volumetric water content is determined empirically in the laboratory. The effect of varying the texture, bulk density, temperature, and soluble salt content on this relationship was also determined. Time-domain reflectometry (TDR) was used to measure the dielectric constant of a wide range of granular specimens placed in a coaxial transmission line. The water or salt solution was cycled continuously to or from the specimen, with minimal disturbance, through porous disks placed along the sides of the coaxial tube.

Four mineral soils with a range of texture from sandy loam to clay were tested. An empirical relationship between the apparent dielectric constant K_a and the volumetric water content θ_v, which is independent of soil type, soil density, soil temperature, and soluble salt content, can be used to determine θ_v from air dry to water saturated, with an error of estimate of 0.013. Precision of θ_v to within ±0.01 from K_a can be obtained with a calibration for the particular granular material of interest. An organic soil, vermiculite, and two sizes of glass beads were also tested successfully. The empirical relationship determined here agrees very well with other experimenters' results, which use a wide range of electrical techniques over the frequency range of 20 MHz and 1 GHz and widely varying soil types. The results of applying the TDR technique on parallel transmission lines in the field to measure θ_v versus depth are encouraging.

INTRODUCTION

Soil water content and the availability of water are fundamentally important to land activities, especially those involving agriculture, forestry, hydrology, and engineering. Knowledge of soil water contents over extensive areas is necessary for use in crop yield optimization and flood control. Currently available methods involve point measurements, which are too costly for extensive use, or remotely sensed techniques, which at best detect only surface conditions.

The neutron moderation technique has come into regular use for monitoring at established sites. The need for site calibration and the inherent radiation hazard make this technique less than ideal. Although the removal of samples and measuring their water content is both direct and reliable, the technique is destructive, time consuming, and thus impractical for large-scale determinations.

An ideal method would use a soil physical property, which is a function primarily of water content and which can be measured directly and reliably. In the frequency range of 1 MHz to 1 GHz, the real part of the complex dielectric constant (K') is not strongly frequency dependent, however, K' appears to be highly sensitive to the volumetric water content (θ_v) and weakly sensitive to soil type and density as discussed by *Nikodem* [1966], *Thomas* [1966], *Lundien* [1971], *Cihlar and Ulaby* [1974], *Hipp* [1974], *Hoekstra and Delaney* [1974], *Davis and Annan* [1977], and *Davis et al.* [1977]. Unfortunately, the reliability of published data that cover this frequency range is dubious, since the systems used for measuring the electrical properties were usually designed either for frequencies up to the MHz range or for frequencies in the microwave region (i.e., down to 1 GHz), and thus the 1-MHz to 1-GHz band was usually at the limit of the measuring systems.

The objective of the work reported here was to establish in the laboratory the dependence of K' on θ_v over this frequency range for a wide range of materials and in particular soils. The time-domain reflectometry technique used is reasonably simple to implement and is analogous to short-pulse radar systems [*Annan and Davis*, 1978], which may also prove to be practical for measuring soil water content rapidly and reliably.

ELECTRICAL PROPERTIES OF SOILS

A general discussion of the electrical properties of heterogeneous materials was given in *de Loor* [1956], *Chernyak* [1964], *van Beek* [1965], *Pearce et al.* [1973], *Selig* [1975], *Davis and Annan* [1977], *Wobschall* [1977], and *Wang and Schmugge* [1978]. These papers convinced us of the complexities of the electrical properties of wet soils and the need for reliable empirical data.

The electrical notation used in this paper is

$$K^* = K' + j\{K'' + (\sigma_{dc}/\omega\epsilon_0)\} \quad (1)$$

where K^* is the complex dielectric constant, K' is the real part of the dielectric constant, K'' is the imaginary part of the dielectric constant or the electric loss, σ_{dc} is the zero-frequency conductivity, ω is the angular frequency, ϵ_0 is the free-space permittivity, and j is $(-1)^{1/2}$. The magnetic properties of virtually all geologic materials do not vary significantly from the magnetic properties of free space. Therefore, the effect of variations in magnetic properties do not have to be considered when making electromagnetic measurements.

The variables which affect the electrical response in soils are texture, structure, soluble salts, water content, temperature, density, and measurement frequency. The most important variable is the excitation frequency. Over the frequency range of 1 MHz to 1 GHz, the real part of the dielectric constant does not appear to be strongly frequency dependent [*Davis and Annan*, 1977]. It is therefore unlikely that there ex-

[1] Now with Ensco Incorporated, Springfield, Virginia.
[2] Now with Barringer Research, Toronto, Canada.

Paper number 9W1751.
0043-1397/80/009W-1751$01 00

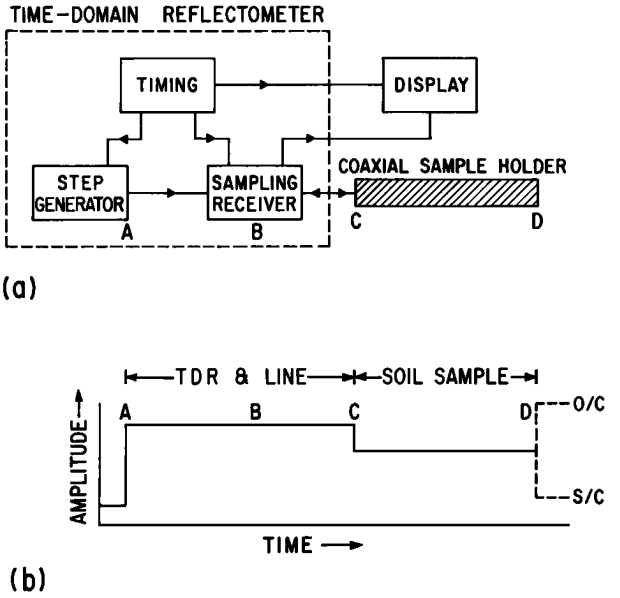

Fig. 1. (*a*) Block diagram of time-domain reflectometer (TDR) connected to soil sample holder. (*b*) An idealized representation of the TDR output from measurement on a soil sample; time interval C–D represents the travel time in the soil sample; O/C, S/C indicate open circuit and short circuit, respectively.

ist any relaxation mechanisms which impart strong temperature dependence to the real dielectric constant K'. *Davis and Annan* [1977] also indicated that the dielectric loss K'' was considerably less than K' in this frequency range.

Experimental Procedures

The experimental procedures are drawn from both electronics and soil science and have been separated into the following categories: (a) the TDR technique, (b) the coaxial transmission line soil column, (c) the soils and other porous media, and (d) the experimental variations applied to the soils.

The TDR Technique

The TDR technique as applied to the measurement of the electrical properties of materials was given in *Fellner-Feldegg* [1969]. A discussion of TDR applied to soils can be found in *Davis and Chudobiak* [1975] and Davis et al. (unpublished manuscript, 1980). Briefly, the propagation velocity (V) of an electromagnetic wave in a transmission line of a known length is determined.

$$V = c \left/ \left(K' \frac{1 + \{1 + \tan^2 \delta\}^{1/2}}{2} \right)^{1/2} \right. \quad (2)$$

where c is the velocity of an electromagnetic wave in free space (3×10^8 m/s) and

$$\tan \delta = \{K'' + (\sigma_{dc}/\omega\epsilon_0)\}/K' \quad (3)$$

If $\tan \delta$ is much less than 1 then

$$V \approx c/(K')^{1/2} \quad (4)$$

For all the soils studied by the authors, to date the electric loss has been small and has not significantly altered the measured propagation velocity. Even though not measurable, the effects of electrical loss did exist in our estimate of K', therefore we called our measured dielectric constant the apparent dielectric constant K_a. Thus for low-loss, nearly homogenous materials

$$K_a \approx K' \quad (5)$$

Figure 1(*a*) is a block diagram of the TDR system. The TDR source generated a fast rise time step function, as shown in Figure 1(*b*) at A. The step propagated down a standard transmission line through the receiver B to the transmission line under test C.

The receiver used an electronic sampling technique to put out a lower-frequency facsimile of the high-frequency input. The sampling principle is analogous to the principle of optical stroboscopes, which are used to make rapidly moving things appear to be at rest or moving very slowly. Many transmitted pulses were generated by the TDR in the time necessary to produce a scan, which was displayed on the record. The timing circuits of the sampling receiver were synchronized with the source. The TDR output consisted of a signal, which was displayed on a cathode ray tube and photographed, or plotted on an x-y plotter, and the data could also be recorded on analog or digital magnetic tape for future signal processing. A number of TDR systems are available. For the readers' benefit we include the name of the TDR system used in this study—Tektronix Model 7S12 TDR sampler with S-52 and S-6 pulse generator and sampling heads in a 7603 oscilloscope main frame.

The transmission line under test, C, usually had different electrical characteristics from the standard transmission line in the TDR, and thus part of the signal was reflected and part of the signal continued down the line to its end D, where all the signal was reflected from either an open or short circuit. Measuring the travel time of the step between C and D and knowing the transmission line length, we determined the propagation velocity V and thus derived K_a. Davis et al. (unpublished manuscript, 1980) discuss the practical details of the electrical responses observed and the interpretation technique used.

The Coaxial Transmission Line Soil Column

A coaxial soil container of 5-cm inside diameter was chosen as a minimum size that would give an adequate sampling of soil conditions when applied to transmission lines in the field. The necessary electrical response was verified by measuring K_a of water (81.5 at 20°C) and K_a of air (1) to better than 2% of reading. Since soil at all water contents measured somewhere between these limiting values, we assumed the trans-

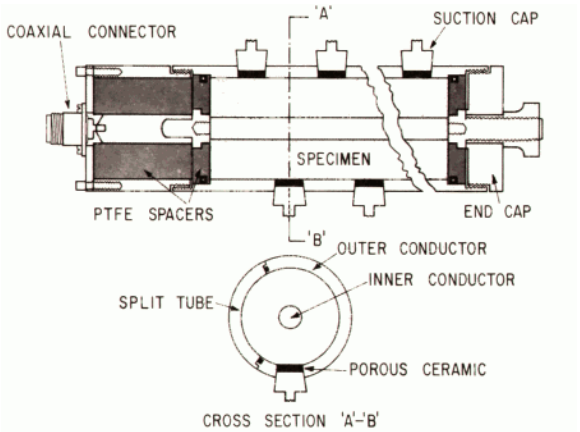

Fig. 2. Diagram of the coaxial transmission line soil column, showing the position relationship of the ceramic-capped cups.

mission line design was adequate for the intermediate values. This meant that these laboratory results could be applied directly to field measurements by using parallel transmission lines with 5-cm spacing [*Davis and Chudobiak,* 1975].

The lengths of the soil in the coaxial lines were either 1.0 m or 0.33 m, depending on the expected electrical loss in the soil under test. In a soil having high electrical attenuation (loss), the shorter transmission line length improved the precision of determining the electrical response from the end of the line.

Water was inserted into or removed from the soil, with minimal disturbance, through 1-cm-diameter porous ceramic disks spaced 5 cm apart on two sides of the coaxial sample holder as shown in Figures 2 and 3. PTFE (polytetrafluoroethylene, also known by the trade name Teflon) disks 1 cm thick were placed at the ends of the sample to hold in the soil and water and to support the center conductor. The water added or removed was measured in burettes with a precision better than 0.5% of the total sample volume (615 cm^3 or 1844 cm^3). The water content throughout the experiment was known to within 1%.

Usually water was added until it just began to flow out of the ends of the sample holder and then dried first under gravity and then suction. The wetting and drying cycles could be repeated as often as desired for any particular experiment. At the end of the final drying cycle the split coaxial soil sample holder was opened in half along its length, and the soil water content was measured, using regular gravimetric techniques. The air dry soil water content of the soil put into the holder was always determined before water was added. The soil density was measured before and after the wetting took place, and it was found that these density measurements agreed to better than 1%, in all cases.

Soils and Other Porous Media

In the initial evaluation of the TDR procedure, four mineral soil materials were chosen to give a wide range of textures (sandy loam to clay) and varying organic matter contents. The particle size distributions and percentages of organic material are listed in Table 1. As a further test of the applicability of these techniques, an organic soil, ground vermiculite mineral, and two sizes of glass beads were also studied. It was assumed that this range of materials, although chemically simpler, individually, than soil, would represent the chemical and physical extremes of pore sizes and surface properties encountered in soil and thus would represent the range of electrical properties given by soil materials. Using materials with well-defined physical properties, e.g., glass beads, allowed technique or equipment comparisons to be carried out.

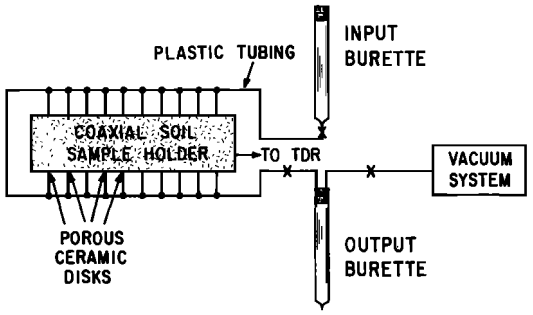

Fig. 3. Diagram of the water input and removal procedure.

The mineral soil materials were taken from the field, dried in air at room temperature, and passed through a 2-mm sieve. The vermiculite mineral was ground to pass through a 0.5-mm sieve. The organic soil was dried at room temperature in air, but was not sieved. All of these porous media, except the organic soil, were packed into the coaxial cylinders by using mechanical vibration of the cylinder, while a rotating funnel carefully deposited material around the center conductor of the coaxial cylinder. This method was a modification of that of *Jackson et al.* [1962] and was found to give very uniform lateral and longitudinal deposition of the materials. The organic soil was packed into the cylinder by manually adding increments of a few grams of soil to the cylinder and packing each one on the last one by using a disc which had clearance on the center conductor and walls of the coaxial cylinder.

Experimental Variations Applied

A series of 18 different experiments were carried out to ascertain the influence of selected parameters on the relationship between water content and apparent dielectric constant. A list of the experiments is presented as rows in Table 2, and variations on the parameters of each experiment are given in the columns.

In column B the size given for glass beads represents the median value, and the bracketed number gives the range of particle sizes. Column F gives the range and cyclic pattern of water content changes applied to each experiment in which the dielectric constant was measured. A sequence of numbers such as 0.018/0.431, 0.192, 0.415 means TDR measurements were made at θ_v = 0.018 (air dry) but not again until θ_v = 0.431, and then at θ_v increments of <0.02, during decreasing water content, to θ_v = 0.192, followed by increasing θ_v to 0.415, etc. Column H indicates the figure in which the data from each experiment have been presented.

The experiments were chosen to find out the effects of texture, bulk density, temperature, salinity, and hysteresis on the

TABLE 1. Soil Type, Particle Size Distribution, and Percentage of Organic Material of the Four Mineral Soils Tested

Soil Type, Depth in Centimeters	Percentage of Clay, <0.002 mm	Percentage of Silt, 0.002–0.05 mm	Percentage of Sand, 0.05–2.0 mm	Percentage of Organic Material	Textural Class
Rubicon (0–20 cm)	9	26	65	3	sandy loam
Bainsville (0–20 cm)	34	36	30	6	clay loam
Bainsville (40–50 cm)	36	42	22	1	clay loam
Bainsville (90–110 cm)	66	31	3	0	heavy clay

TABLE 2. Experiments Performed to Establish the Relationship Between Water Content and Apparent Dielectric Constant

Experiment	Medium	Size or Texture	Depth in Field	Dry Density During Study, gm cm^{-3}	Solution	Water Content, θ_v Range, and Cycles	Date, Duration of Experiment, Days	Data Appear in Figure
1	Rubicon soil	sandy loam	0–20 cm	1.43	0.01 N $CaSO_4$	0.018/0.431, 0.192, 0.415, 0.223	6/16/1976 (11)	4, 5
2	Rubicon soil	sandy loam	0–20 cm	1.44	0.01 N $CaSO_4$	0.02, 0.431, 0.218	4/12/1977 (13)	4, 5, 8
3	Rubicon soil	sandy loam	0–20 cm	1.32	0.01 N $CaSO_4$	0.016, 0.455, 0.336, 0.403, 0.297, 0.407, 0.34	4/22/1977 (30)	4, 5
4	Rubicon soil	sandy loam	0–20 cm	1.38	2000 ppm NaCl	0.022, 0.449, 0.396	9/2/1977 (3)	8
5	Bainsville soil	clay loam	0–20 cm	1.23	0.01 N $CaSO_4$	0.072/0.458, 0.261, 0.439, 0.286	6/24/1976 (15)	4
6	Bainsville soil	clay loam	0–20 cm	1.23	0.01 N $CaSO_4$	0.324		7
7	Bainsville soil	clay loam	40–55 cm	1.04	0.01 N $CaSO_4$	0.069/0.532, 0.348, 0.501, 0.340	7/12/1976 (12)	4
8	Bainsville soil	clay loam	40–55 cm	1.04	0.01 N $CaSO_4$	0.073, 0.526, 0.337	7/23/1976 (8)	4
9	Bainsville soil	clay	90–110 cm	1.14	0.01 N $CaSO_4$	0.058, 0.454, 0.354	7/30/1976 (6)	4
10	Organic soil	n.d.	0–20 cm	0.422	0.01 N $CaSO_4$	0.033, 0.551	10/7/1977 (10)	6
11	Vermiculite	n.d.	n.a.	1.08	0.01 N $CaSO_4$	0.048, 0.539, 0.212	9/16/1977 (8)	6
12	Glass beads	30 μm (10–50)	n.a.	1.51	water	0.35, 0.22	7/22/1977 (8)	6
13	Glass beads	30 μm (10–50)	n.a.	1.51	water	0, 0.318, 0.039, 0.325, 0.124, 0.315, 0.113	5/3/1977 (26)	6
14	Glass beads	30 μm (10–50)	n.a.	1.49	water	0, 0.338, 0.159	6/13/1977 (13)	6
15	Glass beads	30 μm (10–50)	n.a.	1.53	2000 ppm NaCl	0/0.348, 0.116, 0.307, 0.150	8/3/1977 (15)	6
16	Glass beads	450 μm (300–600)	n.a.	1.60	2000 ppm NaCl	0, 0.332, 0.06	7/12/1977 (9)	
17	Glass beads	450 μm (300–600)	n.a.	1.60	water	0, 0.334, 0.046	6/27/1977 (11)	6
18	Glass beads	450 μm (300–600)	n.a.	1.61	water	0, 0.327, 0.061, 0.299, 0.065	5/30/1977 (13)	6

Columns A–G give the value of particular parameters adjusted for each experiment listed in rows.
N.d., not determined; n.a., not available.

relationship between water content θ_v and apparent dielectric constant K_a. In addition it was necessary to check the repeatability of the methods.

For a wide variation in soil materials, the texture and density were interrelated and could not be separated independently for this study. Those experiments whose results display the effect of texture were one from each material tested, e.g., 2, 5, 7, 9, 10, 11, 12, 18. In addition these materials had a wide range of specific surface area and still permitted the introduction and extraction of water. Although a range of density of 1 to 1.6 gm cm^{-3} was obtained for the inorganic materials, this range was not independent of the variation in texture. Experiments 2 and 3, for one soil type, show a 9% difference, which was the maximum range in density attainable while maintaining a uniform density in the sample during changes in water content.

The effect of temperature was studied in experiment 6, where the temperature of the room in which the experiments were carried out was varied from 10°C to 36°C. The water input and output connections to the coaxial cylinder were closed when the soil water content was 0.324. The apparent dielectric constant for this 1 m length of soil was measured at selected temperatures. The temperature of the soil was measured by using thermocouples placed inside the inner conductor and outside the outer conductor. The room, soil, and electronic equipment were allowed 24 hours to stabilize after each temperature change. All other experiments were conducted at a controlled temperature of 20.5°C.

In experiments 4, 15, and 16 the water (a 0.01 N $CaSO_4$ solution) was replaced by a solution containing approximately 2000 parts per million sodium chloride (2.112 gm l^{-1}). These experiments tested the influence of soluble salt on the apparent dielectric constant. Most of the experiments were cycled through changes in water content to determine if hysteretic effects existed in the θ_v versus K_a relationship. To determine the reproducibility of these procedures, duplicate experiments were carried out, e.g., 1 and 2, 7 and 8, 12 to 14, and 17 and 18.

RESULTS AND DISCUSSION

Dielectric Constant Versus Water Content

Figure 4 presents the relationship obtained between apparent dielectric constant K_a and soil water content θ_v, for the four inorganic soil materials. Although these soils varied widely in both density and texture, there was little difference in the K_a versus θ_v relationship from one soil to another. Before discussing the relationship between K_a and θ_v in detail, we shall determine first what effects texture, density, temperature, and soluble salts had on the relationship. We shall also discuss our experimental reproducibility to give evidence of the significance of the data.

Effects of Texture and Density

A comparison of the results of experiment 2 (*), which used a sandy loam soil, with those of experiment 9 (○), which used a clay soil, indicated differences that texture or specific surface area had on the relationship. The clay soil showed a lower K_a at $\theta_v = 0.1$ but a higher K_a when θ_v was increased to 0.40 than was observed for the sandy loam soil. Therefore, for the fine-grained material the K_a versus θ_v relationship showed greater curvature above $\theta_v = 0.1$. A similar effect was observed for vermiculite and the organic soil. A possible cause for this is

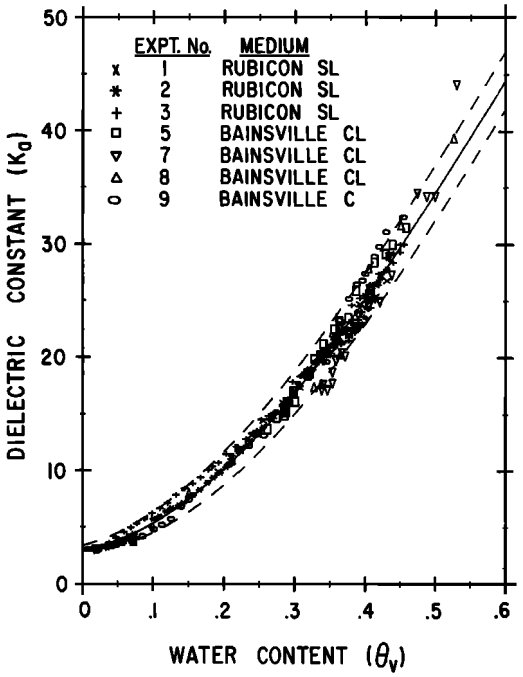

Fig. 4. The measured relationship between K_a and θ_v for the four mineral soils. The solid line is the empirical best-fit equation and the dashed lines are shifted ±0.025 in θ_v. The experiment numbers refer to those used in Table 2.

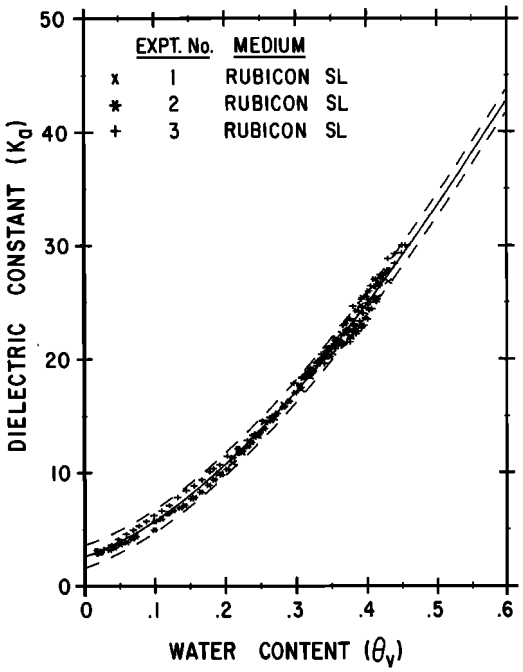

Fig. 5. The measured relationship between K_a and θ_v for the Rubicon soil; the measurements were made at different times and on different subsamples. The solid line is the best-fit equation (see Table 3) and the dashed lines are shifted ±1 in K.

discussed in the section below, entitled Relationship Between K_a and θ_v in Different Materials.

In Figure 5, the data from experiments 1, 2, and 3 show that the 9% change in bulk density of the Rubicon sandy loam soil had no measurable effect on K_a. The error of estimate of K_a for these three experiments combined is 0.56 as shown in Table 3, which is of the same order as the measurement accuracy. Similarly, the data in Figure 4 resulted from soil with density ranging from 1.14 to 1.44 gm cm^{-3}, and it is impossible to identify any effect resulting from density alone.

Experimental Reproducibility

Table 4 lists the third-order polynomial equations derived and the error of estimates of K_a and θ_v for each experiment. The numbers in brackets are the standard deviations of each coefficient. The error of estimate is the square root of the residual variance or the standard deviation of K_a when θ_v is known and vice versa for the error of estimate of θ_v. Table 3 lists the derived equation and error of estimates for a number of combinations of the experiments.

The major source of uncertainty was from the measurement of the travel time on the photograph records, resulting in an error of estimate of ±1 in K_a. The uncertainty of the volumetric water content, owing to evaporation and other water losses during the experiment, was less than ±0.008 in all cases. In an attempt to show the magnitude of the data scatter in relation to these measurement uncertainties, we show in Figure 5 a band whose vertical height is 2 in K_a. This band encompassed most of the data points of the three experiments. When we doubled the error of estimate (the 95% confidence limits) of K_a for the combination of experiments 1, 2, and 3 shown on Table 3, we noted that it was ±1.1, which was similar to the results of our first estimate. Experiments 1 and 2 were carried out 7 months apart in different designs of sample holder and by different experimenters. Tables 3 and 4 show a number of other examples of the excellent experimental reproducibility.

Relationship Between K_a and θ_v in Different Materials

The use of glass beads as a study medium provided, first, the opportunity to study the K_a versus θ_v relationship over a wide range of θ_v, where θ_v could be changed relatively easily; second, a means to measure hysteresis, if any, in the K_a versus θ_v relationship; and third, a relatively easy means to introduce saline solution without the associated problem of changing the physical structure of the study medium, as happened with soil.

The experiments that used the glass beads again demon-

TABLE 3. Equation and Error of Estimate for Combinations of Experiments to Determine the Relationship of K_a versus θ_v

Experiment	Medium	Coefficients of $K_a = A + B\theta_v + C\theta_v^2 - D\theta_v^3$, ± Standard Deviation				Error of Estimate of K_a and θ_v, × 10^{-2}
		A	B	C	D	
1, 2, 3	Rubicon SL	2.59 (±0.16)	21.9 (±1.9)	102 (± 5.6)	44.8 (±3.9)	0.56 0.89
2, 4	Rubicon H_2O and Rubicon NaCl	2.65 (±0.09)	16.5 (±1.1)	123 (± 3.2)	61.0 (±2.3)	0.26 0.83
1, 2, 3, 5, 7, 8, 9	all mineral soils	3.03 (±0.25)	9.3 (±2.8)	146 (± 8.2)	76.7 (±5.7)	1.07 1.3
12, 13, 14	glass, 30 μm	3.79 (±0.25)	41.3 (±3.2)	63.4 (±10.8)	27.0 (±8.0)	0.71 1.07
17, 18	glass, 450 μm	3.57 (±0.21)	31.7 (±2.9)	114 (±10.7)	68.2 (±8.0)	0.71 1.14
12, 13, 14, 17, 18	glass, 30 μm and 450 μm	3.55 (±0.17)	38.0 (±2.2)	84.1 (± 7.9)	44.1 (±5.9)	0.75 1.16

TABLE 4. Equation and Error of Estimate for Each of the Experiments

Experiment	Medium	Coefficients $K_a = A + B\theta_v + C\theta_v^2 - D\theta_v^3$				Error of Estimate of K_a and $\theta_v \times 10^{-2}$
		A	B	C	D	
1	Rubicon SL + H_2O	2.74 (±0.32)	18.2 (± 3.2)	113 (± 9.6)	52.5 (± 6.8)	0.42 0.73
2	Rubicon SL + H_2O	2.56 (±0.14)	16.1 (± 1.7)	127 (± 5.1)	64.4 (± 3.6)	0.32 0.77
3	Rubicon SL + H_2O	2.65 (±0.28)	27.6 (± 3.4)	80.3 (± 9.9)	29.0 (± 7.0)	0.65 0.79
4	Rubicon SL + NaCl	2.87 (±0.15)	15.4 (± 1.8)	125 (± 5.3)	61.8 (± 3.7)	0.28 0.83
5	Bainsville CL + H_2O	2.76 (±0.54)	−1.9 (± 5.4)	196 (±16.0)	115 (±11.3)	0.62 1.2
6	Bainsville CL + H_2O	4.23 (±1.22)	−56.6 (±12.9)	350 (±37.1)	216 (±25.5)	1.43 1.2
8	Bainsville CL + H_2O	2.86 (±1.13)	−2.26 (±11.8)	192 (±33.7)	111 (±23.3)	1.31 1.6
9	Bainsville C + H_2O	3.34 (±0.53)	−7.7 (± 6.4)	222 (±18.6)	136 (±18.8)	0.69 1.1
10	organic soil	1.74 (±0.22)	−0.34 (± 2.3)	135 (± 6.2)	55.3 (± 4.2)	0.38 1.8
11	vermiculite	2.45 (±0.35)	1.8 (± 3.5)	83.1 (± 9.5)	22.2 (± 6.5)	0.63 1.4
12	glass, 30 μm + H_2O	3.62 (±0.26)	41.3 (± 2.9)	59.2 (±10.2)	22.6 (± 7.5)	0.26 0.33
13	glass, 30 μm + H_2O	3.88 (±0.13)	41.3 (± 1.9)	74.5 (± 6.7)	38.1 (± 5.0)	0.35 0.53
14	glass, 30 μm + H_2O	3.03 (±0.17)	43.5 (± 2.1)	49.6 (± 7.0)	14.6 (± 5.1)	0.28 0.46
15	glass, 30 μm + NaCl	3.89 (±0.74)	39.6 (± 8.2)	69.3 (±25.7)	31.3 (±18.4)	0.85 1.3
16	glass, 450 μm + NaCl	3.30 (±0.34)	31.0 (± 5.0)	110 (±18.3)	63.1 (±13.8)	0.84 1.4
17	glass, 450 μm + H_2O	3.33 (±0.25)	32.8 (± 3.7)	116 (±14.7)	70.9 (±10.3)	0.61 1.0
18	glass, 450 μm + H_2O	3.76 (±0.31)	30.5 (± 4.3)	115 (±15.6)	67.8 (±11.7)	0.75 1.2

strated the excellent reproducibility, as shown in Tables 3 and 4 and Figure 6. A possible reason for the slightly greater scatter of data in the 450-μm glass beads was because the water was not distributed as uniformly in the coarse material in the large sample holder. The measured relationship between K_a and θ_v for glass beads was observed to be less curved, especially for the 30-μm beads, than that for the soil material (see the second- and third-order coefficients in Table 4). In addition, there was a vertical displacement of the curve for glass beads, which resulted from a higher K_a (≈3.5) for dry glass beads as opposed to ≈3 for dry soil. The vermiculite and organic soil showed relationships with greater curvature at θ_v up to 0.2 than either glass beads or the other soils. Both the vermiculite and the organic soil showed little measurable change in K_a until θ_v was greater than 0.10. The remainder of these curves was similar to that of the soil material. The dashed lines in Figure 6 enclosed 93% of the data given in Figure 4. These curve shapes gave qualitative confirmation of the hypothesis that the active surface area of the soil controls the dielectric properties of the first few molecular layers of water added to the soil. The first layers, being constrained by the electric field of the soil particles, showed a dielectric constant nearer to that of water constrained in ice structures (i.e., $K' = 3$). Subsequent molecular layers had dielectric constants somewhere between 3 and 81 for liquid water. *Wang and Schmugge* [1978] discuss this further. Inconsistencies in standard laboratory measurements of the surface of the soil materials frustrated attempts to quantify the relationships governing surface area, added water, and measured dielectric constant.

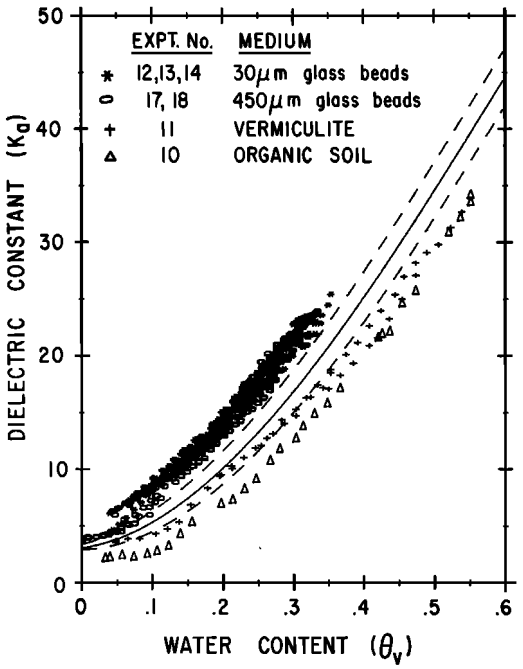

Fig. 6. The measured relationship between K_a and θ_v for the mineral soils, 30 μm glass beads, ground vermiculite, and an organic soil. The area between the dashed lines is the same region as between the dashed lines in Figure 4.

Hysteresis of the K_a vs θ_v Relationship

Although there was little reason to expect hysteresis in the K_a versus θ_v relationship, we did observe some. The separation between wetting and drying branches of a cycle were seldom greater than 2 in K_a and are therefore within the limits of experimental error. An apparent hysteresis was observed with both sizes of glass beads at low water contents. We now believe this was an experimental artifact that resulted from the nonuniformly distributed water during the initial wetting from the porous cups positioned on the outer conductor of the coaxial cylinder. *Annan*'s [1977] calculations indicated that for cases of nonuniform distribution the measured K_a was biased toward the K_a of the material surrounding the inner conductor. Our observations were in accord with those calculations. This factor should be present in all experiments but was only observable with the glass beads that could be dried easily to $\theta_v = 0.05$ or less. The distribution problem of the water occurred mainly on the initial wetting. After an increase of about 0.05 in θ_v, there was no longer any significant effect of unequal water distribution on the measured K_a versus θ_v relationship.

Variations Due to Temperature

The results of experiment 6, to ascertain the influence of temperature, are given in Figure 7. The overall variation of K_a from 10°C to 36°C is less than the experimental error of ±1 shown by the vertical bar at $T = 20.5$°C. *Davis and Annan* [1977] and *Wobschall* [1978] reported that K_a in wet soils did not vary significantly as the temperature was varied from 0° to 30°C.

Variations Due to Change of Soluble Salt Content

A comparison of K_a versus θ_v, from experiments 2 and 4 (Figure 8), shows that the presence of salt in the liquid phase of the soil-water system caused no measurable effect on the apparent dielectric constant. The results for the glass bead experiments were similar. In other words, the dissolved salt did not alter the speed of travel of the voltage step in the medium. However salt did increase the attenuation of the voltage step as it traveled in the soil medium.

Usually more scatter was found in the relationship between K_a and θ_v where salt solution replaced the water. This increasing attenuation effect was not only observed when salt was added to solution, but it was also noted as the soil temperature was increased or as the soil grain size decreased and as the soil water content was increased. A quantitative analysis of the shape of the reflected signal from a known length of soil has the potential of showing the attenuation of the various frequency components of the step pulse.

The TDR technique, being wide band, had the advantage of preferentially using the optimum frequencies in the soil under test, which were a compromise of minimum attenuation and maximum resolution. The attenuation of electromagnetic signals in the wetter soil increased with frequency, and the resolution decreased with decreasing frequency. It is hoped that the data from these experiments can be used to identify the best compromise of frequency for particular soil types. Using a narrower bandwidth system over the optimum frequency range will enable us to increase the signal power into the soil and thus maintain resolution and possibly increase penetration range.

Empirical Relationship Between K_a and θ_v

This study showed that the TDR approach has a great deal of potential, both for further use in the laboratory and in the field. A third-degree polynominal equation was fit to the data from the four mineral soils in Figure 4. The equation for this

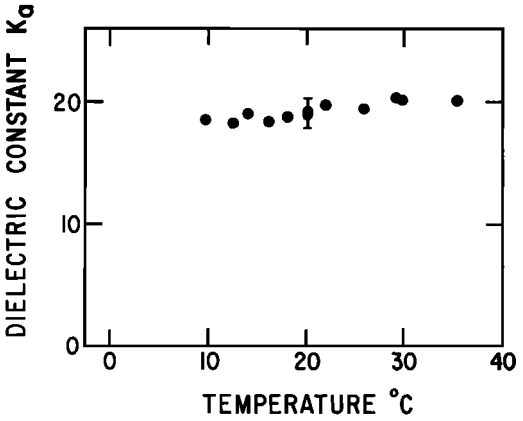

Fig. 7. K_a versus temperature from experiment 6 with Bainsville clay loam surface soil at $\theta_v = 0.324$. The vertical bar at $T = 20$ is ±1 in K_a and represents the measurement precision.

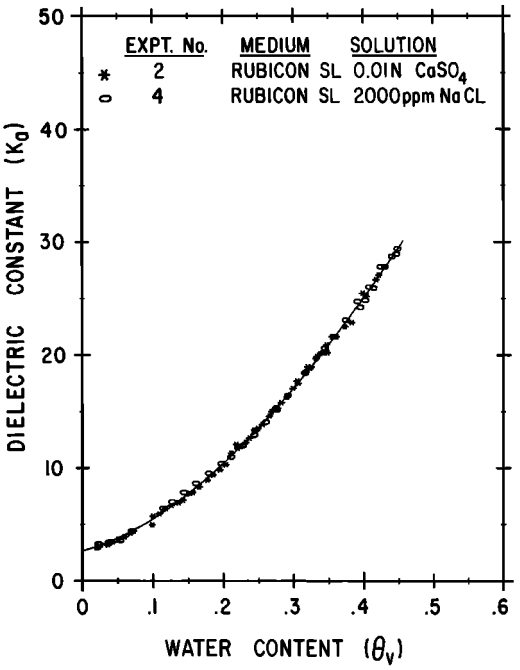

Fig. 8. The measured relationship between K_a and θ_v for the Rubicon soil, where the water solution (0.01 N $CaSO_4$) for experiment 2 was replaced by 2000 ppm NaCl in experiment 4.

line is

$$K_a = 3.03 + 9.3\,\theta_v + 146.0\,\theta_v^2 - 76.7\,\theta_v^3 \quad (6)$$

This equation was constrained to pass through (81.5, 1) the data point for pure water at 20°C. Measurements of K_a versus θ_v for clays at water contents between 0.6 and 0.95 have also been carried out. The data points lie along the empirical curve (6) satisfactorily.

The lines on either side of the data were shifted from the above equation by 0.025 in θ_v, and the band so formed was found to enclose more than 93% of the measured data. Many of the data points falling outside this band occurred at low or high water content extremes, which are less often encountered in the field. Note that the usual statistical methods for determining the confidence limits were not strictly appropriate here because the scatter was due not only to measurement noise but, more significantly, to variations from soil type, soil density, soil temperature, and soluble salts in the water, and therefore, the data were not necessarily normally distributed. If statistical methods were employed as shown in Table 4 for experiments 1, 2, 3, 5, 7, 8, and 9, then doubling the error of estimate gave the 95% confidence limit of 0.026 in θ_v. This result was similar to the nonstatistical technique we first employed because there are a large number of data points. For general application to mineral soil, this curve can be used as an empirical calibration for determination of water content with a standard error of estimate of 0.013 (i.e., 1.3%) over the complete range of water contents (Table 4). Specialized applications requiring greater precision, to the instrumental limit of ±0.01, or using unusual soils require calibration for the particular soil understudy.

In practice we usually measure K_a and want to determine θ_v. The following equation, which uses the same data as (6), assumed K_a was known. To find θ_v, we use

$$\theta_v = -5.3 \times 10^{-2} + 2.92 \times 10^{-2} K_a - 5.5 \times 10^{-4} K_a^2 + 4.3 \times 10^{-6} K_a^3 \quad (7)$$

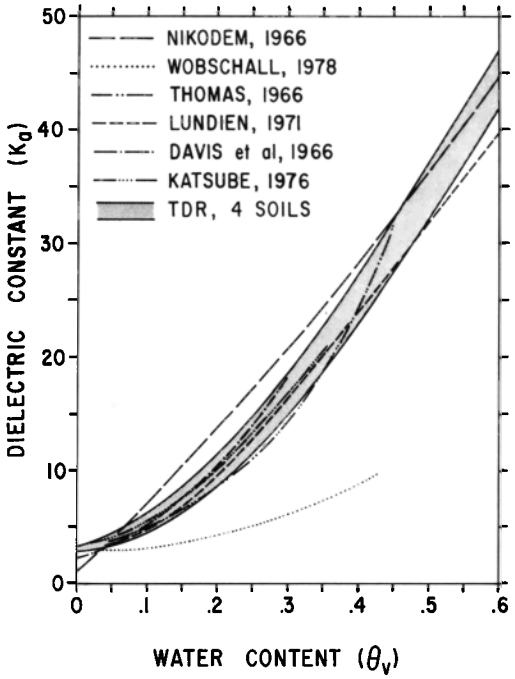

Fig. 9. A comparison of results of the TDR experiments on four different soils possessing a wide range of textures with the results of other experiments which use a variety of techniques and soils.

Comparisons With Other Electrical Measurements

The strong relationship between K_a and θ_v found in these experiments has been observed by other experimenters, using different electrical techniques within the same frequency range. Figure 9 shows a comparison of our TDR experiments on four mineral soils with six other reported experiments that use many different mineral soils and range in frequency from 30 MHz to 1.5 GHz. The data of *Hoekstra and Delaney* [1974] and *Hipp* [1974] were not shown because their data at the lowest experimental frequencies used, 500 MHz and 30 MHz, respectively, gave much higher dielectric constants (up to 12 in dielectric constant at water contents around 0.15 and 0.20) than those shown in Figure 9. Hoekstra and Delaney's data diverged from ours significantly at water contents above 0.1. Both Hoekstra and Delaney's, and Hipp's data points at 4 GHz and 1 GHz, respectively, agreed to within $K_a = \pm 3$ of the empirical curve obtained by using the TDR reported here. It was difficult to explain why the Hoekstra and Delaney data at water contents greater than 0.1 and at 500 MHz, using the TDR technique, did not agree with our data nor with other experimenters' results at 300 MHz and 1 GHz. *Wobschall's* [1978] theoretical curve was lower than any of the other data reported, though his 1977 curve [*Wobschall*, 1977] appeared to fit *Thomas'* [1966] curve at water contents below 0.3. It was clear though that Wobschall's theoretical curve did run low compared to all the experimental data reported. *Selig* [1975] showed many data points of K_a versus θ_v obtained at 20 MHz by three different experimenters, and these fell satisfactorily around our empirical equation over the 0.30 to 0.60 water content range.

It was interesting to note that measurements made at 6 GHz on wet snow samples over a water content range of 0.05 to 0.20 agreed well with the curve given here [*Sweeny and Colbeck*, 1974]. This was not too surprising, since the dielectric constant of ice was 3.15, which was very similar to the dielectric constant of dry soil, 3.0, and the other components of the mixture were the same. At higher water contents Sweeney and Colbeck's curve diverged from ours, which was probably due to the increasing effects of the relaxation mechanisms of the water molecules. It was further evidence that there is a fundamental relationship between the apparent dielectric constant and volumetric water content in wet granular mixtures.

CONCLUSIONS

The results of this study have shown that the apparent dielectric constant is strongly dependent on the volumetric water content of the soil. In addition, the dielectric constant was almost independent of soil density, texture, and salt content. There was no significant temperature dependence. The apparent dielectric constant varied over a range of 3 to 40 for a change in the volumetric water content of 0 to 0.55 in mineral soils. The simplicity of measurement, using time-domain reflectometry, and the empirical equation derived here provide a powerful tool for measuring soil water content rapidly and reliably.

The fact that the results of more than 10 different experimenters, who used widely differing soils, electrical measuring techniques, and frequencies, agreed closely with the empirical curve reported here is further evidence that K_a was strongly dependent on θ_v and only weakly on soil type, density, temperature, and frequency between 20 MHz and 1 GHz. The excellent agreement with other experimenters also showed that TDR is a useful technique for measuring at high frequencies the electrical properties of materials.

Although coaxial transmission lines are inappropriate for field use, the installation of parallel transmission lines are being evaluated as a tool to determine soil water content versus depth. The preliminary results of these experiments are very encouraging as indicated by *Davis et al.* [1977]. Two practical problems require resolution: first, the design of transmission line components for optimum resolution of the dielectric constant with depth in the soil; and second, the development of procedures for installation of the transmission lines so that the lines do not influence the wetting and drying processes in the soil. Both laboratory and field experiments are underway to develop further the application of this technique to obtain rapid reliable measurements of volumetric water content in the field.

Acknowledgments. The authors are grateful to Denis Brûlé, Walter Zebchuk, and Janet Otoroski for their assistance with experiment procedures and data analyses.

REFERENCES

Annan, A. P., Time-domain reflectometry—Air-gap problem in a coaxial line, Report of Activities, Part B, *Pap. 77-1B,* 55–58, Geol. Surv. Can., Ottawa, 1977.

Annan, A. P., and J. L. Davis, High-frequency electrical methods for the detection of freeze-thaw interfaces, *Proc. Third Int. Conf. Permafrost, 1,* 496–500, 1978.

Chernyak, G. Ya., and N. A. Ogih'yi (Ed.), *Dielectric Methods for Investigating Moist Soils* (in Russian), Izdatel' stvo 'Nerdra,' Moskva, 1964. (English translation, 106 pp., Israel Program for Scientific Translations, Jerusalem, 1967.)

Cihlar, J., and F. T. Ulaby, Dielectric properties of soils as a function of moisture content, *RSL Tech. Rep. 177-47,* Univ. Kans. Center Res., Inc., Lawrence, Kansas, 1974.

Davis, B. R., J. L. Lundien, and A. N. Williamson, Feasibility study of the use of radar to detect surface and ground water, *Tech. Rep. 3-727,* U.S. Army Corps of Eng., Vicksburg, Miss., 1966.

Davis, J. L., and W. J. Chudobiak, In-situ meter for measuring relative permittivity of soils, *Pap 75-1A,* pp. 75–79, Geol. Surv. Can., Ottawa, 1975.

Davis, J. L., and A. P. Annan, Electromagnetic detection of soil moisture: Progress report 1, *Can. J. Remote Sensing, 3,* 1, 76–86, 1977.

Davis, J. L., G. C. Topp, and A. P. Annan, Electromagnetic detection of soil water content, Proceedings of the Workshop on Remote Sensing of Soil Moisture and Groundwater, Toronto, Ontario, Canada, November 1976, *Progr. Rep. 2,* pp. 96–109, Can. Aeronaut. Space Inst., Ottawa, Canada, 1977.

de Loor, G. P., Dielectric properties of heterogeneous mixtures, Ph.D. thesis, Univ. of Leiden, 94 pp., Leiden, Holland, 1956.

Fellner-Feldegg, J., The measurement of dielectrics in the time domain, *J. Phys. Chem., 73,* 616–623, 1969.

Hipp, J. E., Soil electromagnetic parameters as a function of frequency, soil density, and soil moisture, *Proc. IEEE, 62,* 98–103, 1974.

Hoekstra, P., and A. Delaney, Dielectric properties of soils at UHF and microwave frequencies, *J. Geophys. Res., 79,* 1699–1708, 1974.

Jackson, R. D., R. J. Reginato, and W. E. Reeves, A mechanical device for packing soil columns, *Publ. 41-52,* Agr. Res. Serv., U.S. Dep. Agr., Washington, D. C., 1962.

Katsube, T. J., Electrical properties of water in rocks and soils, Proceedings of the Workshop on Remote Sensing of Soil Moisture and Groundwater, Toronto, Ontario, Canada, November 1976, report, pp. 110–121, Can. Aeronaut. and Space Inst., Ottawa, Canada, 1977.

Lundien, J. R., Terrain analysis by electromagnetic means, *Tech. Rep. 3-693,* U.S. Army Corps of Eng., Vicksburg, Miss., 1971.

Nikodem, H. J., Effects of soil layering on the use of VHF radio waves for remote terrain analysis, Proceedings of the 4th Symposium on Remote Sensing of Environment, report, pp. 691–703, Univ. Mich., Ann Arbor, 1966.

Pearce, D. C., W. H. Hulse, and J. W. Walker, The applications of the theory of heterogeneous dielectrics to low surface area soil systems, *IEEE Trans. Geosci. Electron., 11,* 167–170, 1973.

Selig, E. T., and S. Mansukhani, Relationship of soil moisture to the dielectric property, *J. Geotech. Eng. Div., Amer. Soc. Civil Eng., 101*(GT8), 755–769, 1975.

Sweeny, B. D., and S. C. Colbeck, Measurements of the dielectric properties of wet snow using a microwave technique, *Res. Rep. 325,* 31 pp., U.S. Army Cold Reg. Res. and Eng. Lab., Hanover, N. H., 1974.

Thomas, A. M., In situ measurement of moisture in soil and similar substances by fringe capacitance, *J. Sci. Instr., 43,* 21–27, 1966.

van Beek, L. K. H., Dielectric behaviour of heterogeneous systems, in *Progress in Dielectrics,* vol. 7, edited by J. B. Birks, pp. 69–114, C.R.C. Press, Boca Raton, Fla., 1965.

Wang, J. R., and T. J. Schmugge, An empirical model for the complex dielectric permittivity of soils as a function of water content, *NASA Tech. Memo. 79659,* 35 pp., Goddard Space Flight Center, Greenbelt, Md., 1978.

Wobschall, D., A theory of the complex dielectric permittivity of soil containing water: The semi-disperse model, *IEEE Trans. Geosci. Electron., 15,* 49–58, 1977.

Wobschall, D., A frequency shift dielectric soil moisture sensor, *IEEE Trans. Geosci. Electron., GE-16,* 2, 112–118, 1978.

(Received July 18, 1979;
revised November 29, 1979;
accepted December 13, 1979.)